SUPPORTING INFORMATION:

Temperature Dependence of the Vibrational Spectrum of Porphycene: A Qualitative Failure of Classical-Nuclei Molecular Dynamics

Yair Litman,[1] Jörg Behler,[2] and Mariana Rossi[1]

[1] *Fritz Haber Institute of the Max Planck Society, Faradayweg 4–6, 14195 Berlin, Germany.*

[2] *Universität Göttingen, Institut für Physikalische Chemie, Theoretische Chemie, Tammannstr. 6, 37077 Göttingen, Germany.*

(Dated: 19 June 2019)

I. BASIS SETS COMPARISON

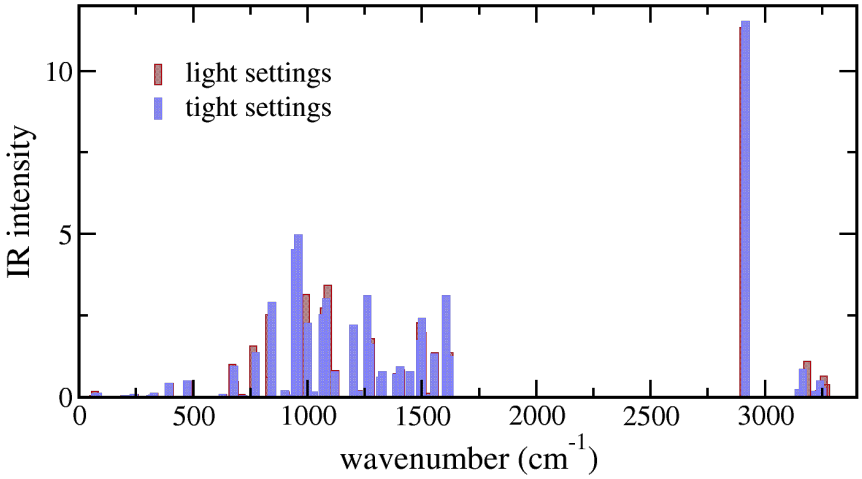

FIG. S1: Comparison of harmonic IR spectra of gas-phase Pc-*d*0 calculated with the B3LYP+vdW functional using light and tight numerical and basis-set settings of the FHI-aims code package[1]. Differences in peak positions amount to maximally 20 cm^{-1}.

II. NEURAL NETWORK POTENTIAL AND KERNEL RIDGE REGRESSION TESTS

A. Fitting accuracy

In Fig. S2, the HDNNP energies of the full structures-set are compared with the reference DFT energies. As can be observed, for HDNNP A, B and F all points lie close to the line with slope 1, which corresponds to a perfect fit. For HDNNP C, D and E the deviations from the perfect line above 200 meV is considerable. This behavior is not surprising because those HDNNPs were not trained with path integral MD data, which ultimately proves the necessity to include those data points in the training set.

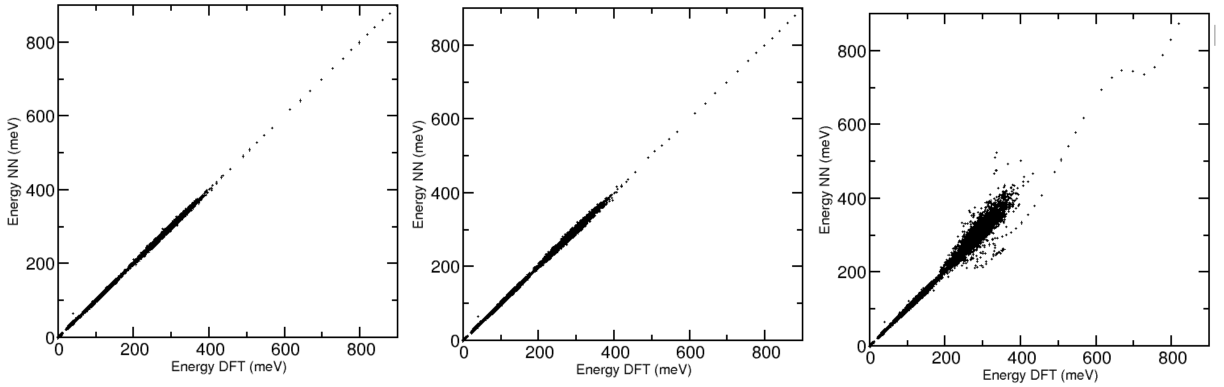

(a) HDNNP A (b) HDNNP B (c) HDNNP C

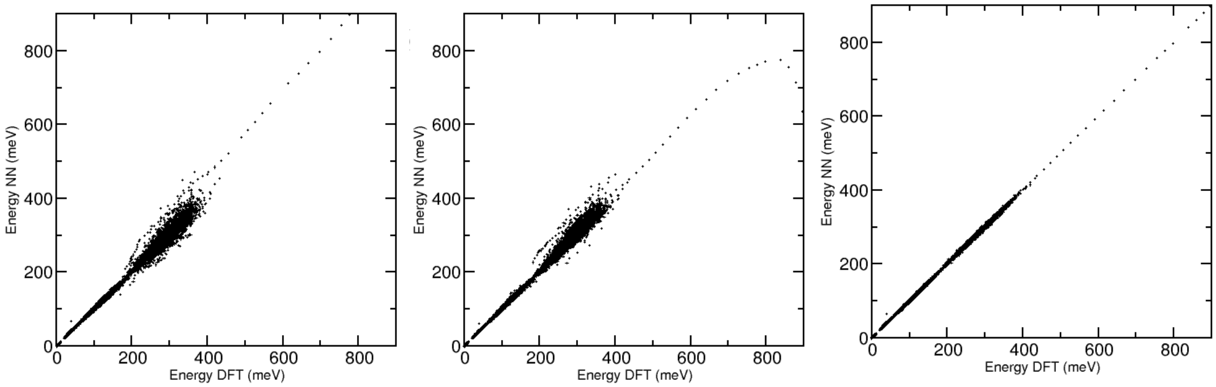

(d) HDNNP D (e) HDNNP E (f) HDNNP F

FIG. S2: Comparison of the DFT and high dimension neural network potential (HDNNP) energies for the full structures set. Only the HDNNP F was trained with the full set (see Table 2 in the main manuscript.)

B. Static values

In Table SI we show the energy and nitrogen-hydrogen stretch frequencies for all the stationary points obtained with DFT and the high dimensional neural network potential (HDNNP). In Table SII we show the corresponding nitrogen-nitrogen (d(NN)) and hydrogen-nitrogen (d(NH)) distances. For all cases the error in the distances is smaller or equal than 0.005 Å.

#	DFT	A	B	C	D	E	F	G
Cis	93	103	95	103	105	90	104	105
SD1	189	205	200	205	203	197	194	192
SD2	290	314	316	315	317	306	295	293
Neg. Freq SD1	1228	1252	1283	1314	1286	1270	1233	1236
Neg. Freq SD2 (1)	1263	1266	1283	1307	1318	1284	1262	1262
Neg. Freq SD2 (2)	1126	1141	1165	1199	1195	1143	1113	1113
Freq N-H stretch (trans)	2903	2888	2937	2929	2921	2916	2922	2908
Freq N-H stretch (trans)	2907	2901	2945	2938	2933	2940	2929	2916
Freq N-H stretch (cis)	2678	2603	2678	2605	2615	2714	2668	2622
Freq N-H stretch (cis)	2640	2567	2659	2670	2669	2803	2685	2660

TABLE SI: Relative energies of stationary points of the PES with respect to the *trans* conformational minima (first three rows), as well as and relevant harmonic vibrational frequencies. SD1 and SD2 refer to first and second order saddle point structure. Frequencies are expressed in cm^{-1} and energies in meV.

#	DFT	A	B	C	D	E	F	G
Trans d(NH)	1.046	1.045	1.043	1.045	1.045	1.046	1.044	1.044
Trans d(NN)	2.647	2.643	2.647	2.641	2.643	2.642	2.644	2.642
Cis d(NH)	1.061	1.065	1.059	1.060	1.062	1.058	1.059	1.061
Cis d(NN)	2.608	2.597	2.602	2.602	2.602	2.610	2.607	2.061
SD2 d(NN)	2.495	2.495	2.494	2.491	2.500	2.492	2.490	2.490

TABLE SII: Nitrogen-hydrogen (d(NH)) and nitrogen-nitrogen (d(NN)) distances along the hydrogen bond for all the stationary points. Distances are expressed in Å.

C. Hydrogen transfer rates

In Table SIII we show the hydrogen transfer rates obtained for selected HDNNP following the procedure described in Ref.[2].

#	DFT	A	B	F	G
Concerted 100K	1.99	1.06	2.15	1.35	1.19
Stepwise 100K	0.13	0.07	0.12	0.06	0.05
Total 100K	2.25	1.20	2.39	1.47	1.29
Relative error	-	**-50 %**	**+6 %**	**-35 %**	**-42 %**
Concerted 150K	4.67	2.62	5.80	3.62	3.12
Stepwise 150K	1.90	1.20	2.18	1.22	1.15
Total 150K	8.47	5.02	10.16	5.06	4.42
Relative error	-	**-40%**	**+20 %**	**-40 %**	**-47 %**

TABLE SIII: Hydrogen transfer rates k for concerted and stepwise double-hydrogen transfer mechanisms. Rates expressed in $10^{11}s^{-1}$. Relative error (RE) defined as RE $= k_{\mathrm{NN}}/k_{\mathrm{DFT}} - 1$. For the sake of comparison, no correction of the barrier height data was applied here.

D. Equilibrium time-independent properties

In Fig. S3 we show the comparison of the quantum potential energy probability density at 290K between DFT and the HDNNP ensemble.

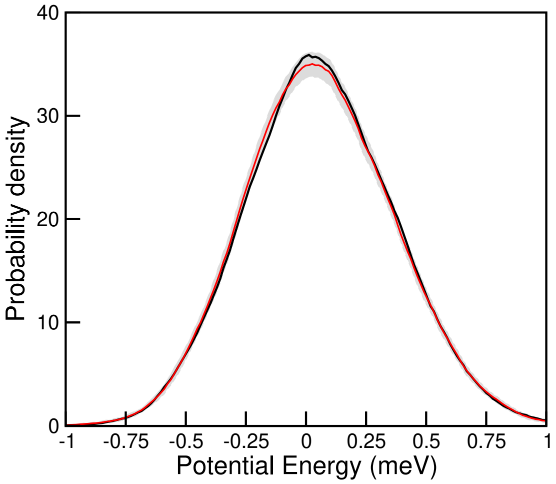

FIG. S3: Potential energy probability density at 290K obtained from a TRPMD run simulated with DFT (black curve) and the HDNNPs. The HDNNP values are expresses as a mean value over all the HDNNPs (red curve) with the corresponding standard deviation (grey area).

E. Equilibrium time-dependent properties and combination with KRR model

In Fig. S4 we show the velocity density of states (VDOS) at 290K for DFT and selected HDNNPs. There is an overall good agreement between the different HDDNPs and DFT, except for the region between 750-1000 cm^{-1}. In this interval, also the HDNNPs differ to each other. This result suggest that in order to better reproduce this frequency interval the data set should be extended.

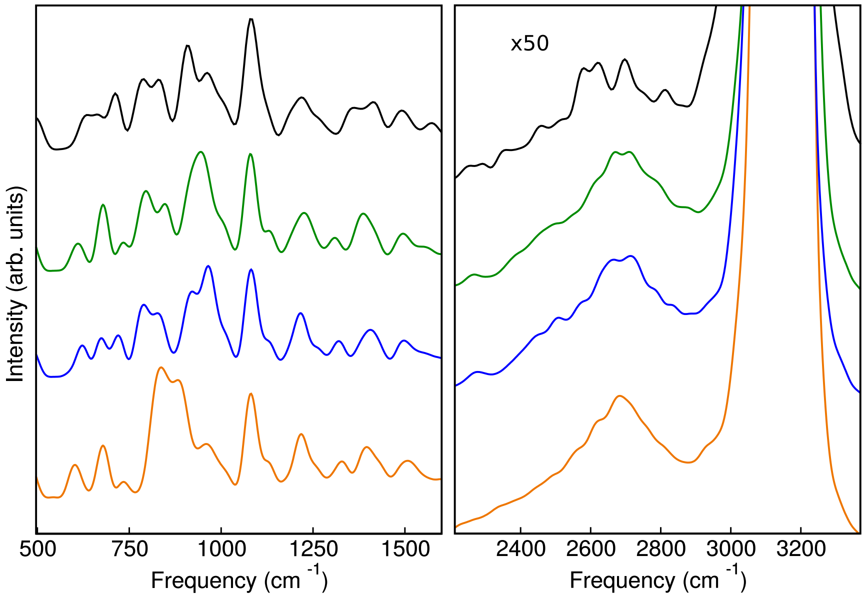

FIG. S4: VDOS at 290K obtained from TRPMD simulated with DFT (black), HDNNP B (dark green), HDNNP A (blue) and HDNNP F (orange).

In Fig. S5 we show the IR spectra obtained with TRPMD at 290K for DFT and selected HDNNPs. It can be seen again an overall good agreement between the different HDDNPs and DFT. Discrepancies appear around 1250 cm^{-1}, but in this case the three HDNNPs give a consistent result. In order to understand whether this difference comes from the HDNNP or the KRR model, we show in Fig. S6 the collective VDOS (CVDOS) as defined in Ref.[3], in which cross terms involving different degrees of freedom are included. The difference between the IR and CVDOS comes only from the dipole selection rules and eventual non-linear dependencies of the dipoles with respect to positions, but it is a much closer quantity to the IR than the VDOS. As can be observed in Fig. S6, the agreement between DFT and HDNNPs is much better, which shows that errors in the KRR model are responsible for the discrepancy. Since the discrepancy in both VDOS and IR spectra takes place on small and localized regions that are not main focus of this paper, we decided to not improve further the HDNNPs.However, these errors in the low frequency region may be the responsible for lack of agreement of the fine structure in the NH vibration peak.

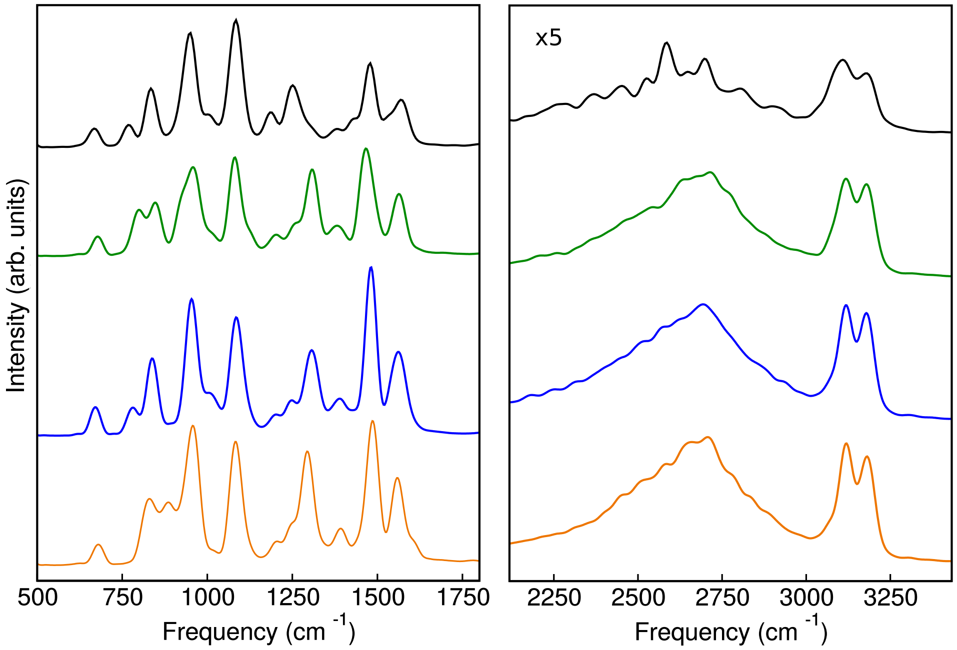

FIG. S5: IR spectra at 290K obtained from TRPMD simulated with DFT (black), HDNNP B (dark green), HDNNP A (blue) and HDNNP F (orange).

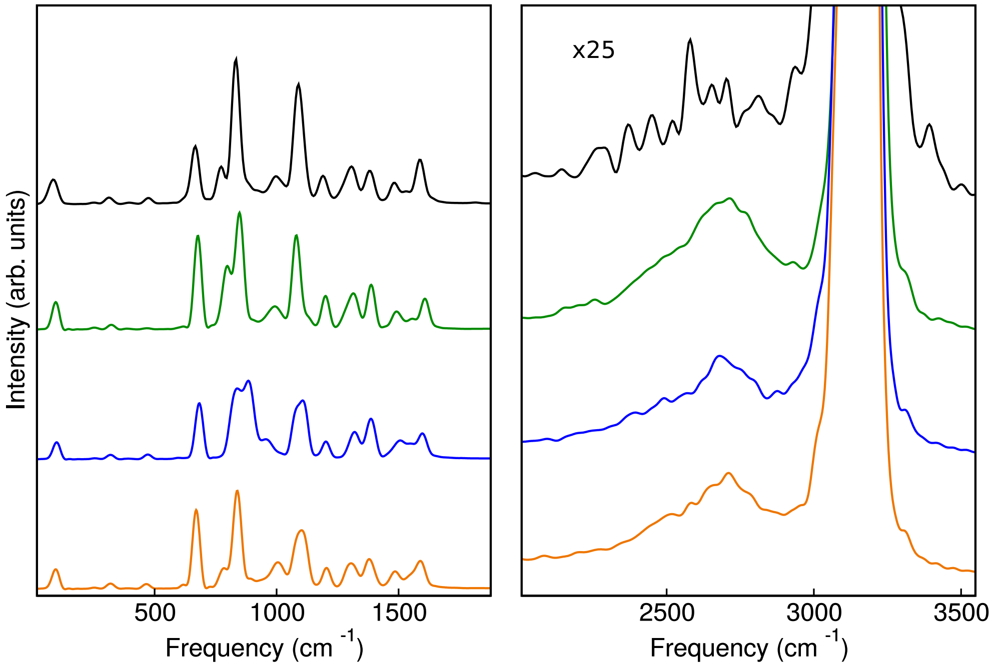

FIG. S6: CVDOS as defined in Ref[3] at 290K obtained from TRPMD simulated with DFT (black), HDNNP B (dark green), HDNNP A (blue) and HDNNP F (orange).

F. KRR model

Fig. S7 shows the comparison between the DFT and the KRR-predicted IR spectra in the exact same trajectory (calculated with DFT forces). The grey areas in the figure show the uncertainty of the model. The agreement is quite good and the uncertainty seems to be very small, especially at lower frequencies. This trajectory was partially included in the training set and the uncertainty (standard deviation) was calculated by randomly selecting different points for the training set. Since these training sets are ultimately correlated, the uncertainty is artificially underestimated in this case.

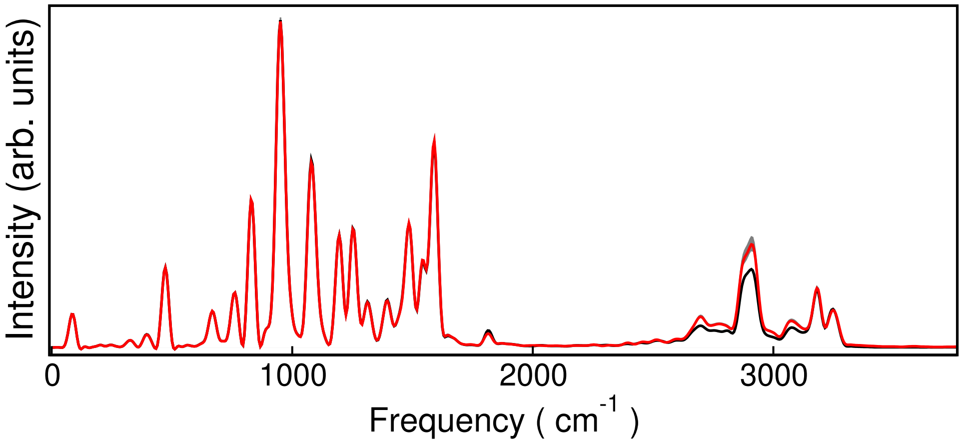

FIG. S7: IR spectrum calculated from DFT dipoles (black) and dipoles predicted by the KRR model (red) based in the same DFT ab initio MD trajectories. Grey area represents the standard deviation of the different KRR models.

III. EQUILIBRIUM GEOMETRICAL PROPERTIES

Equilibrium nitrogen-nitrogen probability density distributions are reported in Fig. S8. As reported in the main text it can be observed the shift towards higher distance with the increase of the temperature. Additionally, an overall broadening in the quantum distribution with respect to the classical one is observed.

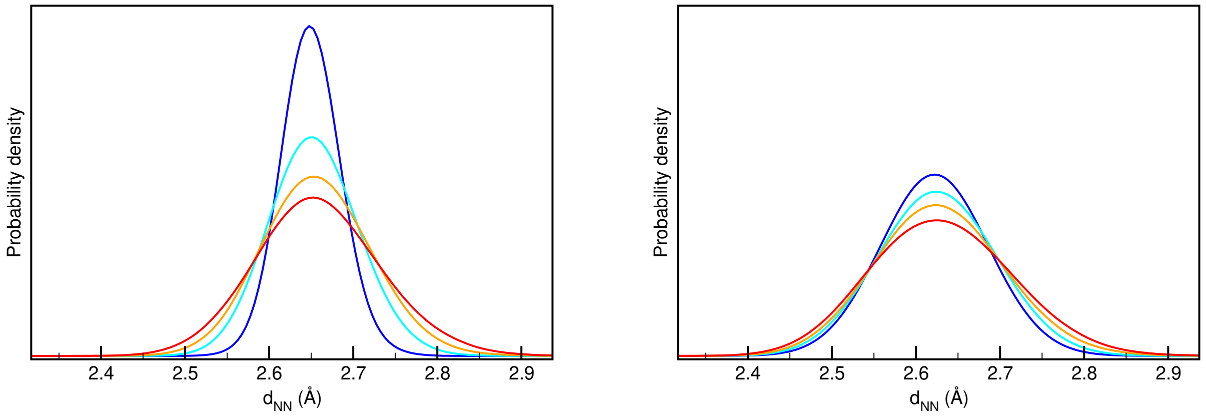

(a) MD

(b) Path integral MD

FIG. S8: Probability distribution of the nitrogen-nitrogen distance at 100 K (blue), 200 K (cyan), 300 K (orange) and 400K (red)

IV. FULL FREQUENCY RANGE IR AND VDOS SPECTRA

The quantum and classical IR spectra for Pc-*d*0 and Pc-*d*12 are shown in Fig. S9 and S10 respectively. As mentioned in the main text, the observed temperature induced frequency shifts are in close agreement with the corresponding ones observed in the VDOS, which is also shown in its full range in Figs. S11 and S12. All data was obtained with HDNNP B and the KRR model.

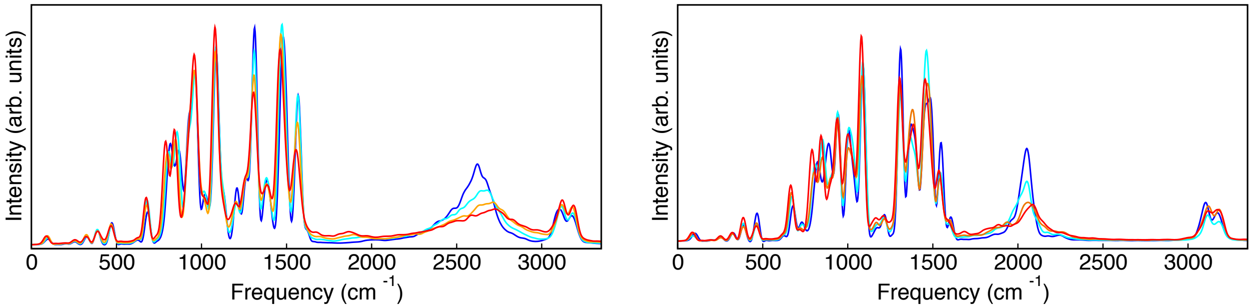

(a) Pc-*d*0

(b) Pc-*d*2

FIG. S9: IR spectra obtained from TRPMD simulations at 100 K (blue), 200 K (cyan), 300 K (orange) and 400K (red).

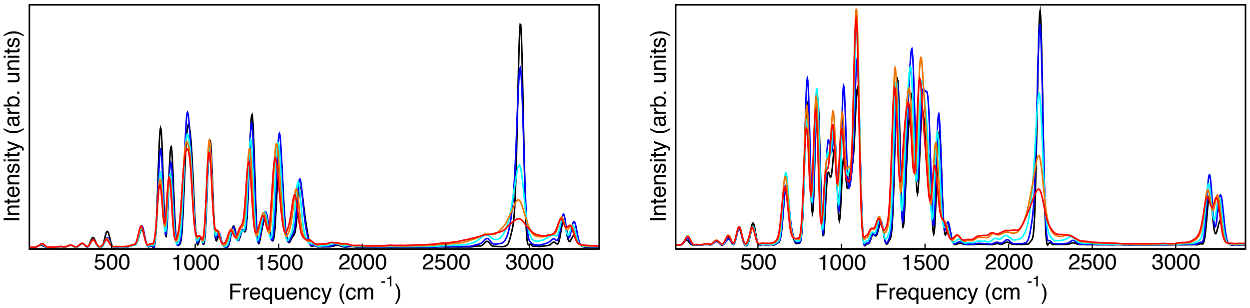

(a) Pc-*d*0

(b) Pc-*d*2

FIG. S10: IR spectra obtained from MD simulations at 50 K (black), 100 K (blue), 200 K (cyan), 300 K (orange) and 400K (red).

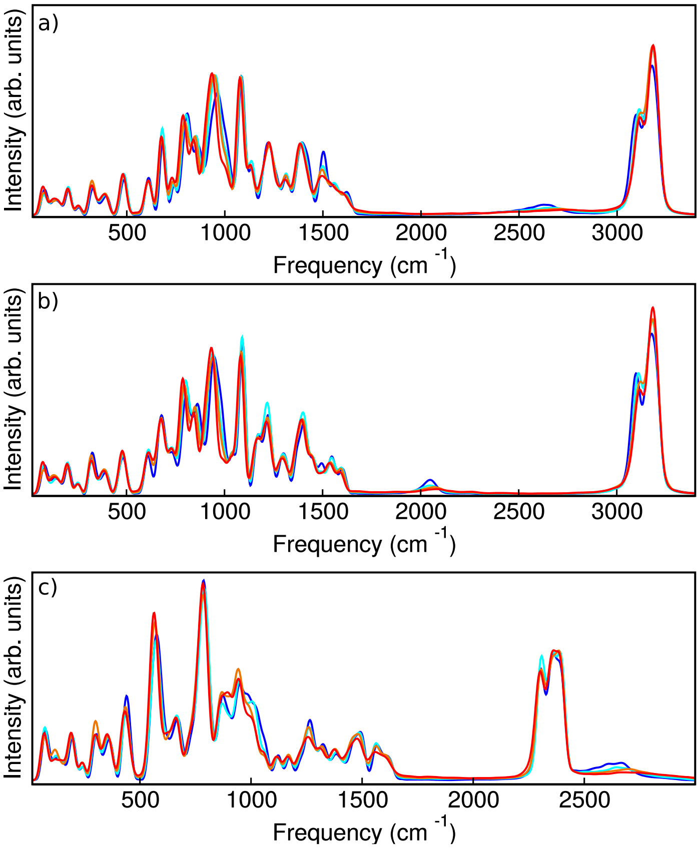

FIG. S11: VDOS in the full range for (a) Pc-*d*0, (b) Pc-*d*2 and (c) Pc-*d*12 obtained with TRPMD, same color code as above.

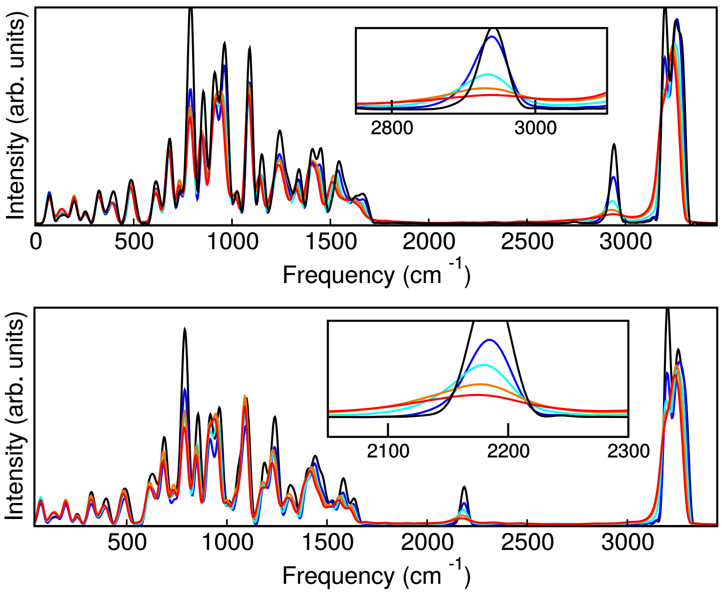

FIG. S12: VDOS in the full range for (top) Pc-*d*0, (bottom) Pc-*d*2 obtained with classical nuclei MD, same color code as above (black is 50 K).

V. VIBRATIONAL PERTUBATION THEORY CALCULATIONS

We performed second-order vibrational perturbation theory (VPT2) calculations using reported standard procedures[4–6] with the HDNNP. We have calculated the whole procedure through 5-point finite differences, since we did not derive an analytical expression for the Hessian from the HDNNP. In Table SIV we show the harmonic and anharmonic frequencies for the 12 CH stretching modes.

Mode #	ω_i (cm^{-1})	ν_i (cm^{-1})
98	3190	3049
99	3196	3097
100	3197	3090
101	3228	3099
102	3229	3100
103	3249	3122
104	3249	3118
105	3265	3127
106	3266	3148
107	3286	3164
108	3286	3147

TABLE SIV: Harmonic (ω_i) and anharmonic (ν_i) CH stretch frequencies obtained by harmonic and VPT2 calculations respectively.

For all CH-stretch modes, we find the most intense couplings (greater than 10 cm^{-1}) at lower frequencies to various CH-bending modes lying between 775 cm^{-1} to 1096 cm^{-1}.

REFERENCES

[1] V. Blum, R. Gehrke, F. Hanke, P. Havu, V. Havu, X. Ren, K. Reuter, and M. Scheffler, Comput. Phys. Commun. **180**, 2175 (2009).

[2] Y. Litman, J. O. Richardson, T. Kumagai, and M. Rossi, J. Am. Chem. Soc. **141**, 2526 (2019).

[3] J. Martí, E. Guàrdia, and J. A. Padró, The Journal of Chemical Physics **101**, 10883 (1994).

[4] S. Califano, *Vibrational States* (John Wiley & Sons) pp. 266–302.

[5] V. Barone, J. Chem. Phys. **122**, 014108 (2005).

[6] J. M. L. Martin, T. J. Lee, P. R. Taylor, and J. François, The Journal of Chemical Physics **103**, 2589 (1995).